IEEE Access
Multidisciplinary | Rapid Review | Open Access Journal

Received September 28, 2018, accepted October 6, 2018, date of publication October 10, 2018, date of current version October 31, 2018.

Digital Object Identifier 10.1109/ACCESS.2018.2875146

Uneven Power Amplifier Shuffling for Space-Time Line Code Systems

JINGON JOUNG[1], (Senior Member, IEEE), AND JIHOON CHOI[2], (Senior Member, IEEE)
[1]School of Electrical and Electronics Engineering, Chung-Ang University, Seoul 06974, South Korea
[2]School of Electronics and Information Engineering, Korea Aerospace University, Goyang 10540, South Korea

Corresponding author: Jihoon Choi (jihoon@kau.ac.kr)

This work was supported by the National Research Foundation of Korea (NRF) grants funded by the Korean Government (MSIP) under Grant NRF-R2016R1D1A1B03930250 and Grant NRF-2016R1A2B4013418.

ABSTRACT In this paper, a novel power amplifier (PA) shuffling method is proposed for a space-time line code (STLC) system with uneven PA gains. The proposed method is composed of pre-shuffling and post-shuffling, which represent the assignment of STLC symbols to PAs and the allocation of PAs to transmit antennas, respectively. Through these shuffling procedures, the proposed scheme matches the larger gain PA to the larger effective channel gain with STLC in order to maximize the STLC decoding signal-to-noise ratio (SNR). A theoretical analysis provides a formula to compute the decoding SNR, and it is shown through numerical simulations that the proposed PA shuffling method can significantly improve the performance of conventional STLC systems, regardless of the channel state information uncertainty, especially when the number of transmit antennas is large.

INDEX TERMS Space-time line code, power amplifier shuffling, asymmetric power amplifier.

I. INTRODUCTION

An antenna shuffling (Ant-S) transmitter maps the coded data streams to the proper antennas according to the shuffling pattern selected by feedback information from the receiver. The Ant-S can substantially improve the received signal-to-noise ratio (SNR) and the throughput of multi-antenna systems, such as double space-time transmit diversity (DSTTD) systems [1], [2] and quasi-orthogonal space-time block code (STBC) systems [3], [4]. On the other hand, asymmetric power amplifiers (PAs) with uneven gains are employed for high energy efficiency [5]–[7]. The uneven PA gains can also be caused by an unintentional impairment of analog parts [8], such as impedance mismatches and/or signal reflections. When the PAs have uneven gains at an orthogonal-STBC system, the Ant-S method can also improve the energy efficiency [9] as well as the spectral efficiency [10].

Recently, a space-time line code (STLC) was proposed to achieve full-spatial-diversity gain [11]–[14], as a counterpart of the STBC. The STLC transmitter encodes the information symbols by using channel state information (CSI), so that the receiver can achieve full spatial diversity just by combining the received signal without the full CSI. The full-spatial-diversity schemes including the STLC completely cover four communication scenarios/configurations. For example, the full-spatial-diversity achieving schemes with the diversity order two are categorized as shown in Fig. 1 and summarized as follows (refer to [11] and [12] for details):

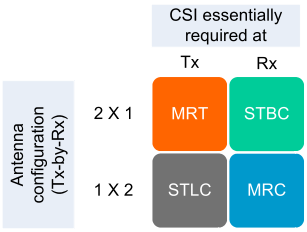

FIGURE 1. Categorization of full-spatial-diversity schemes when the maximum diversity order is two.

- Maximum ratio combining (MRC): using 1×2 antenna configuration, CSI is available only at the receiver (Rx) [15]–[19].
- Maximum ratio transmission (MRT): using 2×1 antenna configuration, CSI is available only at the transmitter (Tx) [20]–[22].
- STBC: using 2×1 antenna configuration, CSI is available only at the Rx [23]–[26].
- STLC: using 1×2 antenna configuration, CSI is available only at the Tx [11]–[14].

Along with the full-spatial-diversity gain of the STLC method, the STLC provides various merits, such as the

complexity reduction of the receiver [11], interference mitigation [12], [14], and peak-to-average-power ratio reduction under per-antenna power constraints [13].

In this paper, motivated by the Ant-S and STLC, we devise a novel PA shuffling (PA-S) method to further improve the performance of STLC systems that employ the uneven PAs. To allocate PAs to the proper effective channels with the STLC, pre- and post-shuffling matrices are required before and after the PAs, respectively. It is shown that the pre- and post-shuffling matrices are the symmetric binary matrices. The shuffling matrix is optimally designed to maximize the STLC decoding SNR, and it is revealed out that the optimal strategy for PA allocation is to map a larger gain PA to the large effective channel gain after STLC decoding process. Since the CSI is basically assumed to be available at the STLC transmitter [11], [12], [14], the allocation can be readily found at the STLC transmitter without any additional feedback or signaling process. However, additional switches are required to implement the PA-S, and thus the switch insertion loss is inevitable [27]–[30]. Nevertheless, as verified by numerical results, the proposed PA-S method can significantly improve the bit-error-rate (BER) performance of the conventional STLC system that does not employ the PA-S. Furthermore, performance degradation caused by CSI uncertainty has been investigated. Two types of uncertainties are considered: i) the CSI estimation error at the transmitter under a time division duplex (TDD) mode and ii) the CSI quantization error at a receiver for the feedback to a transmitter under a frequency division duplex (FDD) mode. Numerical results verify that the proposed PA-S STLC outperforms the conventional STLC, regardless of the type of channel uncertainties. In summary, the main contributions of this study are listed as follows:

- A novel PA-S method composed of pre- and post-shuffling procedures is proposed.
- An optimal PA-S strategy is designed to maximize the STLC decoding SNR. It is shown that the optimal PA-S matches the mth largest PA gain to the mth largest effective channel gain of the STLC, for $1 \leq m \leq M$, where M is the number of transmit antennas.
- A formula is derived to compute the theoretical decoding SNR of the proposed optimal PA-S method.
- Through numerical simulations, it is verified that the proposed PA-S scheme can significantly improve the BER performance, regardless of the CSI uncertainty that caused by the channel estimation errors or quantization errors.

Notation: Throughout the paper, for any vector or matrix, the superscripts $*$ and T denote complex conjugate transposition and transpose, respectively; the notation $\|\boldsymbol{x}\|$ denotes the two norm (Euclidean norm) of vector $\boldsymbol{x}$; $\boldsymbol{I}_m$ and $\boldsymbol{0}_m$ represent an m-by-m identity and zero matrices, respectively; $x \sim \mathcal{CN}(0, \sigma^2)$ means that a complex random variable x conforms to a normal distribution with a zero mean and variance σ^2; and E stands for the expectation of a random variable.

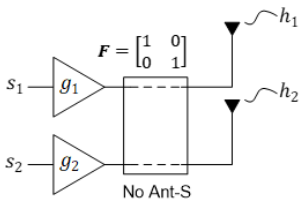

FIGURE 2. Ant-S (post-shuffling) when antennas are not shuffled.

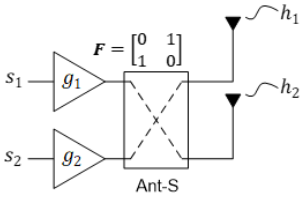

FIGURE 3. Ant-S (post-shuffling) when antennas are shuffled.

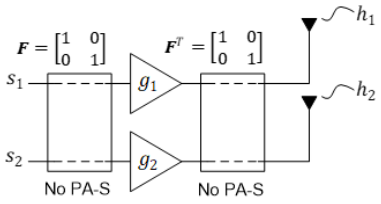

FIGURE 4. PA-S (pre- and post-shuffling) when PAs are not shuffled.

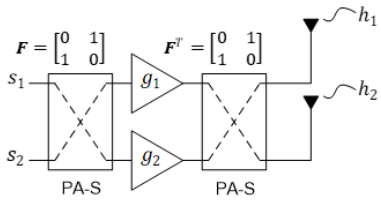

FIGURE 5. PA-S (pre- and post-shuffling) when PAs are shuffled.

II. POWER AMPLIFIER SHUFFLING METHOD

In this section, we introduce a new PA-S scheme, when two transmit antennas are connected to two PAs with uneven gains. Different from a conventional transmit antenna shuffling method (e.g., [2], [9], [10]), which requires post-shuffling after the amplification, the PA shuffling requires pre- and post-shuffling procedures described as $\boldsymbol{F}$ and $\boldsymbol{F}^T$. The shuffling matrix $\boldsymbol{F} \in \mathbb{R}^{M \times M}$ is defined as

$$\boldsymbol{F} = \begin{bmatrix} \boldsymbol{f}_1 & \boldsymbol{f}_2 & \cdots & \boldsymbol{f}_M \end{bmatrix}^T, \tag{1}$$

where $\boldsymbol{f}_m \in \mathbb{R}^{M \times 1}$ is a binary vector such that $\sum_{i=1}^{M} f_{i,m} = 1$, i.e., only one element is '1' and the others are '0's. If $\boldsymbol{F} = \boldsymbol{I}_M$, the PA-S is deactivated. For clarification, the conventional Ant-S, the new PA-S, and no shuffling cases are presented in Figs. 2–5, where two encoded symbols s_1 and s_2 are transferred through two transmit antennas. The transmitter has two PAs, PA1 and PA2, whose gains are g_1 and g_2, respectively. From Figs. 2–5, we can readily obtain the received signals from two transmit antennas, u_1 and u_2, for each case as follows:

(a) $u_1 = s_1 g_1 h_1$ and $u_2 = s_2 g_2 h_2$ (no Ant-S)
(b) $u_1 = s_1 g_1 h_2$ and $u_2 = s_2 g_2 h_1$ (Ant-S)
(c) $u_1 = s_1 g_1 h_1$ and $u_2 = s_2 g_2 h_2$ (no PA-S)
(d) $u_1 = s_1 g_2 h_1$ and $u_2 = s_2 g_1 h_2$ (PA-S)

Here, we see that the Ant-S switches the channel gains, while the PA-S switches the PA gains. Comparing (a) and (c), it is obvious that no Ant-S and no PA-S are identical to each other. On the other hand, suppose that $g_1 \neq g_2$. Then, whether (b) and (d) are identical or not depends on how s_1 and s_2 are generated, i.e., the encoding scheme. If the encoded symbols s_1 and s_2 are independent of the channel gains, which is assumed in conventional systems, (b) and (d) are identical to each other, and the Ant-S for orthogonal STBC systems using uneven PAs is a good example [10]. However, if s_1 and s_2 are encoded by using the channel gains h_1 and h_2, (b) and (d) can be different, i.e., the Ant-S and PA-S methods have different performances. Clearly, the Ant-S is a special case of the PA-S. Note that the PA-S is also different from the PA switching that switches or selects PAs for a single antenna before the amplification (see [5], [6]).

III. PROPOSED PA-S FOR STLC SYSTEMS

Consider an STLC system that consists of a transmitter with M antennas and a receiver with two antennas, as illustrated in Fig. 6. There are M PAs with uneven gains at the transmitter, and they are shuffled according to the matrix $\boldsymbol{F}$ in (1). Denote the index of a nonzero element of $\boldsymbol{f}_m$ be $i_m \in \mathcal{M} = \{1, 2, \ldots, M\}$. Then, i_m should satisfy the following conditions C1 and C2 from the definition of $\boldsymbol{F}$:

C1. $i_m \neq i_{m'}$, if $m \neq m'$.
C2. $\bigcup_{m=1}^{M} \{i_m\} = \mathcal{M}$.

The transmitter constructs the shuffling matrix $\boldsymbol{F}$ (or equivalently $\{i_m\}$) which is designed using the CSI.

In the following subsections, we define the signal model for an STLC system with PA-S, derive the maximum likelihood (ML) decoding method, and finally, propose a design method for the shuffling matrix $\boldsymbol{F}$.

A. SIGNAL MODEL FOR PA-S-BASED STLC

Let $h_{n,m}$ be the channel gain between the mth transmit antenna and the nth receive antenna, where $m \in \mathcal{M}$ and $n \in \mathcal{N} = \{1, 2\}$. The channel $h_{n,m}$ is an independent and identically distributed (i.i.d.) complex Gaussian random variable with zero mean and unit variance, i.e., $h_{n,m} \sim \mathcal{CN}(0, 1)$.

Let us define $\boldsymbol{x} = [x_1, x_2]^T \in \mathbb{C}^{2\times 1}$ as the information symbols transferred through the $2 \times M$ channel, where $E[x_1] = E[x_2] = 0$ and $E[\boldsymbol{x}\boldsymbol{x}^H] = \boldsymbol{I}_2$. When the STLC is used, the transmitter generates the symbols encoded for the mth transmit antenna, using the CSI of $\boldsymbol{h}_m = [h_{1,m},\ h_{2,m}]^T \in \mathbb{C}^{2\times 1}$, as follows [11], [12]:

$$\begin{bmatrix} s_{1,m}^* \\ s_{2,m} \end{bmatrix} = \frac{1}{\|\boldsymbol{h}_m\|} \begin{bmatrix} h_{1,m} & h_{2,m} \\ h_{2,m}^* & -h_{1,m} \end{bmatrix} \begin{bmatrix} x_1^* \\ x_2 \end{bmatrix}, \quad \forall m \in \mathcal{M}, \tag{2}$$

where $s_{t,m}$ is the STLC symbol transmitted through the mth transmit antenna at time t, such that $\mathrm{E}\left|s_{t,m}\right|^2 = 1,\ \forall m \in \mathcal{M}$.

The mth PA gain including the gain variation at multiple transmit RF chains is denoted as g_m, and the PA gain matrix $\boldsymbol{G}$ is defined as

$$\boldsymbol{G} = diag(g_1, g_2, \cdots, g_M). \tag{3}$$

Without loss of generality, it is assumed that the PA gains are sorted in descending order; i.e., $g_1 \geq g_2 \geq \cdots \geq g_M$.

When the proposed PA-S method is applied to the STLC system, $\boldsymbol{s}_t = [s_{t,1}, \cdots, s_{t,M}]^T \in\in \mathbb{C}^{M\times 1}$ is multiplied by the matrices $\boldsymbol{F}$, $\boldsymbol{G}$, and $\boldsymbol{F}^T$, and the resultant signal vector $\boldsymbol{u}_t = \boldsymbol{F}^T\boldsymbol{G}\boldsymbol{F}\boldsymbol{s}_t \in\in \mathbb{C}^{M\times 1}$ is transmitted through M antennas at time t, where $t = 1, 2$. Consequently, the Consequently, the received signal at time t is denoted as

$$\begin{aligned} \boldsymbol{y}_t &= [y_{t,1}, y_{t,2}]^T \\ &= \boldsymbol{H}\boldsymbol{u}_t + \boldsymbol{w}_t \\ &= \boldsymbol{H}\boldsymbol{F}^T\boldsymbol{G}\boldsymbol{F}\boldsymbol{s}_t + \boldsymbol{w}_t, \end{aligned} \tag{4}$$

where $y_{t,n}$ is the received signal at the nth antenna at time t; the channel matrix $\boldsymbol{H} = [\boldsymbol{h}_1, \boldsymbol{h}_2, \cdots, \boldsymbol{h}_M]$; and $\boldsymbol{w}_t = [w_{t,1}, w_{t,2}]^T$ is an i.i.d. complex additive white Gaussian noise (AWGN) vector with zero mean and variance σ_w^2, i.e., $\boldsymbol{w} \sim \mathcal{CN}(\boldsymbol{0}, \sigma_w^2\boldsymbol{I}_2)$.

B. DECODING FOR PA-S-BASED STLC

From (4), the PA-S matrices can be expressed as

$$\begin{aligned} \boldsymbol{F}^T\boldsymbol{G}\boldsymbol{F} &= [\boldsymbol{f}_1, \boldsymbol{f}_2, \cdots, \boldsymbol{f}_M] \begin{bmatrix} g_1 & 0 & \cdots & 0 \\ 0 & g_2 & \ddots & \vdots \\ \vdots & \ddots & \ddots & 0 \\ 0 & \cdots & 0 & g_M \end{bmatrix} \begin{bmatrix} \boldsymbol{f}_1^T \\ \boldsymbol{f}_1^T \\ \vdots \\ \boldsymbol{f}_M^T \end{bmatrix} \\ &= \sum_{m=1}^{M} g_m \boldsymbol{f}_m \boldsymbol{f}_m^T. \end{aligned} \tag{5}$$

Clearly, we see that the PA-S matrix $\sum_{m=1}^{M} g_m \boldsymbol{f}_m \boldsymbol{f}_m^T$ is a diagonal matrix whose i_mth diagonal element is g_m. Substituting (5) into (4), the receive signal vector is rewritten as follows:

$$\begin{aligned} \begin{bmatrix} y_{t,1} \\ y_{t,2} \end{bmatrix} &= \begin{bmatrix} \boldsymbol{h}_1 & \cdots & \boldsymbol{h}_M \end{bmatrix} \sum_{m=1}^{M} g_m \boldsymbol{f}_m \boldsymbol{f}_m^T \boldsymbol{s}_t + \boldsymbol{w}_t \\ &= \sum_{m=1}^{M} g_m \boldsymbol{h}_{i_m} s_{t,i_m} + \boldsymbol{w}_t, \ t \in \{1, 2\}, \quad m \in \mathcal{M}. \end{aligned} \tag{6}$$

By substituting (2) into (6), the received signals are denoted as follows:

$$y_{1,1} = \sum_{m=1}^{M} \frac{g_m h_{1,i_m}}{\|\boldsymbol{h}_{i_m}\|} \left(h_{1,i_m}^* x_1 + h_{2,i_m}^* x_2^*\right) + w_{1,1}, \tag{7a}$$

$$y_{1,2} = \sum_{m=1}^{M} \frac{g_m h_{1,i_m}}{\|\boldsymbol{h}_{i_m}\|} \left(h_{2,i_m}^* x_1^* - h_{1,i_m}^* x_2\right) + w_{1,2}, \tag{7b}$$

$$y_{2,1} = \sum_{m=1}^{M} \frac{g_m h_{2,i_m}}{\|\boldsymbol{h}_{i_m}\|} \left(h_{1,i_m}^* x_1 + h_{2,i_m}^* x_2^*\right) + w_{2,1}, \tag{7c}$$

$$y_{2,2} = \sum_{m=1}^{M} \frac{g_m h_{2,i_m}}{\|\boldsymbol{h}_{i_m}\|} \left(h_{2,i_m}^* x_1^* - h_{1,i_m}^* x_2\right) + w_{2,2}. \tag{7d}$$

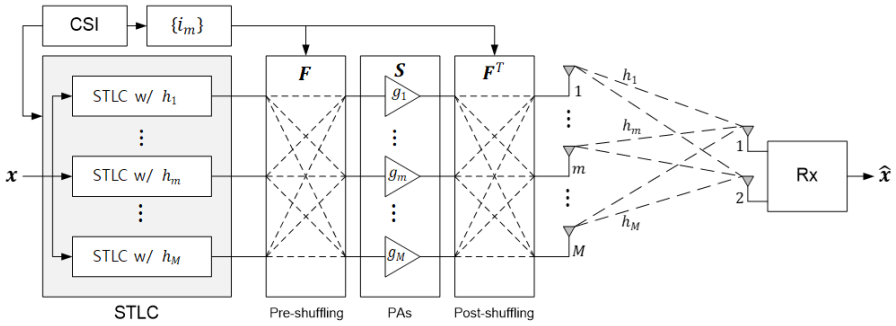

FIGURE 6. Proposed PA-S-based STLC system with uneven gains. The mth PA has gain g_m, where $g_1 \geq g_2 \geq \cdots \geq g_M$.

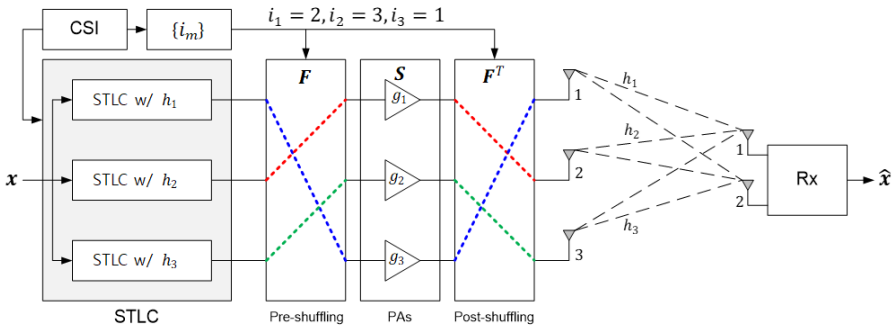

FIGURE 7. Example of the proposed PA-S-based STLC system with $M = 3$ when $g_1 \geq g_2 \geq g_3$ and $\|\boldsymbol{h}_2\| > \|\boldsymbol{h}_3\| > \|\boldsymbol{h}_1\|$.

Then, the receiver combines the received signals in (7) for the STLC decoding as follows [11]–[13]:

$$y_{1,1} + y_{2,2}^* = \lambda(i_m)x_1 + w_{1,1} + w_{2,2}^*, \tag{8a}$$
$$-y_{1,2} + y_{2,1}^* = \lambda(i_m)x_2 - w_{1,2} + w_{2,1}^*, \tag{8b}$$

where $\lambda(i_m)$ is the effective channel gain defined as

$$\lambda(i_m) = \sum_{m=1}^{M} g_m \|\boldsymbol{h}_{i_m}\|. \tag{9}$$

From the combined signals (8a) and (8b), x_1 and x_2 can be separately recovered by the ML detection. Here, note that the effective channel gain $\lambda(i_m)$ is not required for phase-shift keying (PSK) modulated symbol detection, while it is obtained through blind estimation [31] or informed by the transmitter for general modulation schemes.

C. PROPOSED PA-S METHOD

Now, we design the PA-S matrix $\boldsymbol{F}$ to maximize the instantaneous decoding SNR in (8). The SNR maximization problem with respect to $\boldsymbol{F}$, equivalently $\{i_m\}$, is formulated as follows:

$$\{i_m^o\} = \max_{i_m \in \mathcal{M}} \frac{\lambda(i_m)^2}{2\sigma_w^2} \tag{10a}$$
$$\text{s.t. } i_m \neq i_n, \text{ if } m \neq n, \quad \bigcup_{m=1}^{M} \{i_m\} = \mathcal{M}. \tag{10b}$$

As shown in Appendix, the SNR in (10a) is maximized when g_m is mapped to the transmit antenna with the mth largest channel gain. Remind that $g_1 \geq g_2 \geq \cdots g_M$. Precisely, the optimal i_m^o is defined as the order of $\{\|\boldsymbol{h}_m\|\}$ when sorted in descending order. For example, if $M = 3$ and $\|\boldsymbol{h}_2\| > \|\boldsymbol{h}_3\| > \|\boldsymbol{h}_1\|$, the PA-S indices will be $i_1 = 2$, $i_2 = 3$, and $i_3 = 1$, such that the STLC signals generated with $\boldsymbol{h}_2$, $\boldsymbol{h}_3$, and $\boldsymbol{h}_1$ will be amplified with gains g_1, g_2, and g_3, respectively, as depicted in Fig. 7. The fundamental role of the PA-S is the same as that of the Ant-S in [2], [9], and [10], in which the PA with the larger gain is assigned to the assigned to the transmit antenna with the larger channel gain. In the PA-S, the PA with the larger gain is mapped through pre-shuffling and post-shuffling to the STLC symbol and the transmit antenna, respectively, which have the larger effective channel gain for the STLC.

D. SNR ANALYSIS OF PROPOSED PA-S METHOD

To derive the theoretical SNR for the proposed optimal PA-S method, we define

$$Y = \sum_{m=1}^{M} g_m \left\| \sqrt{2}\boldsymbol{h}_{i_m} \right\|. \tag{11}$$

Suppose that the PA gains $\{g_m\}$ are fixed. Since $h_{n,m} \sim \mathcal{CN}(0, 1)$, $\|\sqrt{2}\boldsymbol{h}_{i_m}\|$ follows the Chi distribution with four degrees of freedom. Therefore, from the order statistics,

the probability density function (PDF) of the sorted channel norm $Z_m = \|\sqrt{2}\boldsymbol{h}_{i_m}\|$ is denoted as

$$f_{Z_m}(z) = \frac{M!}{(m-1)!(M-m)!}[1-F_Z(z)]^{m-1}[F_Z(z)]^{M-m}f_Z(z), \tag{12}$$

where $F_Z(z)$ and $f_Z(z)$ are the cumulative distribution function (CDF) and PDF of the Chi distribution with four degrees of freedom, respectively, which are given by

$$F_Z(z) = \frac{\gamma(2, z^2/2)}{\Gamma(2)}, \tag{13a}$$

$$f_Z(z) = \frac{z^3 e^{-z^2/2}}{2\,\Gamma(2)}, \quad z \geq 0. \tag{13b}$$

Here, $\gamma(\cdot,\cdot)$ and $\Gamma(\cdot)$ are the incomplete and complete gamma functions, respectively. Then, the mean squares of Y is derived as follows:

$$E[Y^2] = \left(\sum_{m=1}^{M} g_m E[Z_m]\right)^2 + \sum_{m=1}^{M} g_m^2 \,\mathrm{Var}[Z_m], \tag{14}$$

where $\mathrm{Var}[X]$ means the variance of X, which can be evaluated by only numerical integrations as there is no closed form expression of them. Theoretical SNR is then be obtained by dividing $E[Y^2]$ by $4\sigma_w^2$ as follows:

$$\begin{aligned}\mathsf{SNR} &= \mathrm{E}\left(\frac{\lambda(i_m)^2}{2\sigma_w^2}\right) \\ &= \frac{1}{2\sigma_w^2}\left(\left(\sum_{m=1}^{M} g_m E\left[\|\boldsymbol{h}_{i_m}\|\right]\right)^2 + \sum_{m=1}^{M} g_m^2 \,\mathrm{Var}\left[\|\boldsymbol{h}_{i_m}\|\right]\right).\end{aligned} \tag{15}$$

The analysis is verified through numerical comparison in Section IV. Unfortunately, since closed-form solutions are not available for $E[Z_m]$ and $\mathrm{Var}[Z_m]$, the mean and variance of Z_m need to be evaluated by numerical integrations using (12) and (13). Moreover, the theoretical SNR can be obtained by dividing $E[Y^2]$ by $4\sigma_w^2$. As a special case, when the PA-S is not used, the theoretical SNR in (15) is computed in a closed-form as

$$\mathsf{SNR} = \frac{\frac{2\Gamma(2.5)^2}{\Gamma(2)^2}\left(\sum_{m=1}^{M} g_m\right)^2 + \left(4 - \frac{2\Gamma(2.5)^2}{\Gamma(2)^2}\right)\sum_{m=1}^{M} g_m^2}{4\sigma_w^2}. \tag{16}$$

E. CSI UNCERTAINTY

By virtue of the channel reciprocity in a TDD system, the CSI can be estimated at the transmitter by using the pilot/training signals conveyed from the receiver. In a real system, however, the reciprocity could be generally violated due to the impairment of radio frequency (RF) circuits [32], [33] and the asymmetric interference. Furthermore, the transmitter estimates the full CSI by using the conventional channel estimation methods, such as a minimum mean square error (MMSE) estimator, using pilot/training signals transferred from the receiver, resulting in the CSI estimation error. We denote an uncertain CSI at the transmitter by $\tilde{h}_{n,m} \triangleq h_{n,m} + \epsilon$, where ϵ is the uncertainty or estimation error denoted as independent and identically distributed (i.i.d.) zero-mean Gaussian random variables with variance σ_ϵ^2. This model is valid when the orthogonal pilot sequences are used for the MMSE-based channel estimation [34]. Here, the MSE of the uncertainty is represented as σ_ϵ^2, i.e. $\mathrm{E}\,|h_{n,m} - \tilde{h}_{n,m}|^2 = \sigma_\epsilon^2$ [11], [12].

When STLC symbols in (2) are transmitted using the CSI estimate $\tilde{h}_{n,m}$, the received signals in (7) are rewritten as

$$\tilde{y}_{1,1} = \sum_{m=1}^{M} \frac{g_m h_{1,i_m}}{\|\tilde{\boldsymbol{h}}_{i_m}\|}\left(\tilde{h}_{1,i_m}^* x_1 + \tilde{h}_{2,i_m}^* x_2^*\right) + w_{1,1}, \tag{17a}$$

$$\tilde{y}_{1,2} = \sum_{m=1}^{M} \frac{g_m h_{1,i_m}}{\|\tilde{\boldsymbol{h}}_{i_m}\|}\left(\tilde{h}_{2,i_m}^* x_1^* - \tilde{h}_{1,i_m}^* x_2\right) + w_{1,2}, \tag{17b}$$

$$\tilde{y}_{2,1} = \sum_{m=1}^{M} \frac{g_m h_{2,i_m}}{\|\tilde{\boldsymbol{h}}_{i_m}\|}\left(\tilde{h}_{1,i_m}^* x_1 + \tilde{h}_{2,i_m}^* x_2^*\right) + w_{2,1}, \tag{17c}$$

$$\tilde{y}_{2,2} = \sum_{m=1}^{M} \frac{g_m h_{2,i_m}}{\|\tilde{\boldsymbol{h}}_{i_m}\|}\left(\tilde{h}_{2,i_m}^* x_1^* - \tilde{h}_{1,i_m}^* x_2\right) + w_{2,2}, \tag{17d}$$

and the combined received signals for decoding x_1 and x_2 are denoted as

$$\tilde{y}_{1,1} + \tilde{y}_{2,2}^* = \tilde{\lambda}(i_m)x_1 + \zeta(i_m)x_2^* + w_{1,1} + w_{2,2}^*, \tag{18a}$$

$$-\tilde{y}_{1,2} + \tilde{y}_{2,1}^* = \tilde{\lambda}(i_m)x_2 - \zeta(i_m)x_1^* - w_{1,2} + w_{2,1}^*, \tag{18b}$$

Here, $\tilde{\lambda}(i_m)$ and $\zeta(i_m)$ are the effective and the inter-symbol-interference (ISI) channel gains, respectively, which are written as follows:

$$\tilde{\lambda}(i_m) = \sum_{m=1}^{M} \frac{g_m}{\|\tilde{\boldsymbol{h}}_{i_m}\|}(h_{1,i_m}\tilde{h}_{1,i_m}^* + \tilde{h}_{2,i_m}h_{2,i_m}^*), \tag{19a}$$

$$\zeta(i_m) = \sum_{m=1}^{M} \frac{g_m}{\|\tilde{\boldsymbol{h}}_{i_m}\|}(h_{1,i_m}\tilde{h}_{2,i_m}^* - \tilde{h}_{1,i_m}h_{2,i_m}^*). \tag{19b}$$

Assuming that the receiver operates without recognizing the CSI error at the transmitter, and using the estimated effective channel gain, i.e., $\tilde{\lambda}(i_m) \approx \sum_{m=1}^{M} g_m\|\tilde{\boldsymbol{h}}_{i_m}\|$, x_1 and x_2 are separately demodulated. Compared to the perfect CSI case, the receiver performance is degraded because the channel uncertainty causes the effective channel gain mismatch and the ISI at the receiver. In general, the performance degradation of STLC by CSI error is identical to that of STBC [11].

The STLC receiver only requires the knowledge about the effective channel gain $\tilde{\lambda}(i_m)$. On the other hand, an FDD-based STLC encoder necessitates CSI estimation at the receiver and CSI feedback to the transmitter [35], [36]. However, if the amount of feedback bits is prohibitively huge, for example, the massive MIMO systems [41]–[44], the feedback information needs to be limited to reduce the feedback overhead. To this end, a codebook-based feedback [35], [37]–[40] and a direct quantization of the CSI can be considered. Note

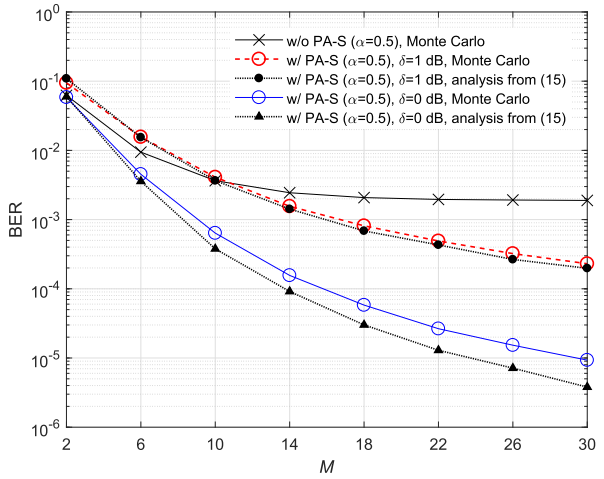

FIGURE 8. BER performance of STLC systems when $1/\sigma_w^2 = 8$ dB. The exponential PA profile and 16-QAM are used and $\alpha = 0.5$.

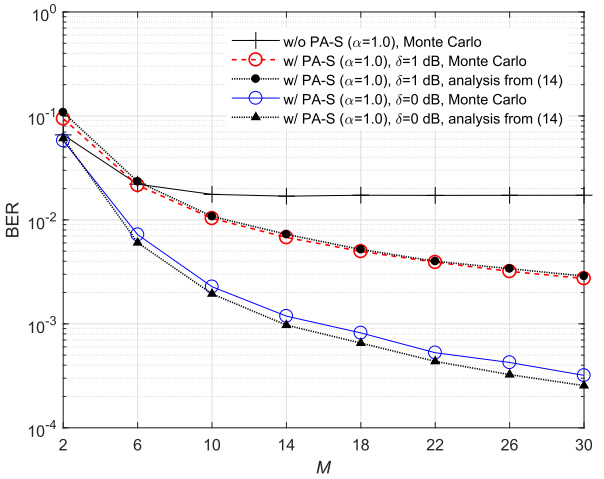

FIGURE 9. BER performance of STLC systems when $1/\sigma_w^2 = 8$ dB. The exponential PA profile and 16-QAM are used and $\alpha = 1$.

that the CSI obtained from the limited feedback information has also uncertainty at the transmitter.

In Section IV-B, numerical results will verify that the proposed PA-S STLC outperforms the conventional STLC in both TDD and FDD modes with CSI uncertainty.

IV. SIMULATION RESULTS

In this section, we evaluate the BER of the proposed PA-S schemes for STLC systems. For BER simulations, quadrature amplitude modulation (QAM) is used. To generate uneven PA gains, we consider an exponential profile [10]: $g_m = \eta \exp(-\alpha(m - M))$, where η is a normalization factor such that $\sum_{m=1}^{M} g_m^2 = 1$, i.e., the total transmit power is one regardless of M, and α is a parameter representing the variation of the PA gains. If $\alpha = 0$, the profile provides even PA gains. As α increases, the PA gains become more uneven. For fairness, an additional switch insertion loss for post-shuffling, δ, is considered for the proposed PA-S-based STLC. From our survey, the insertion loss varies from 0.7 dB to 2 dB [27]–[30]. In our simulation, we set $\delta = 1$ dB if the insertion loss exists.

A. PA-S WITH PERFECT CHANNEL STATE INFORMATION

In the simulation of this subsection, perfect CSI is assumed for the PA-S and STLC.

Figs. 8 and 9 show the BER performance across the number of transmit antennas M, when $1/\sigma_w^2 = 8$ dB and 16-QAM is used. As shown in the results, the SNR analytical results from (15) match well with the Monte Carlo simulation results, especially when the switch insertion loss is nonzero ($\delta = 1$ dB), which is a typical and practical case of interest. Here, note that the insertion loss can be directly applied to the SNR analysis in (15) by substituting g_m with $g_m\delta$. The proposed PA-S method can effectively exploit the increased channel dimension, i.e., spatial diversity, by optimally allocating the PAs to the STLC symbols and the transmit antennas according to the effective channel gains. This is verified from

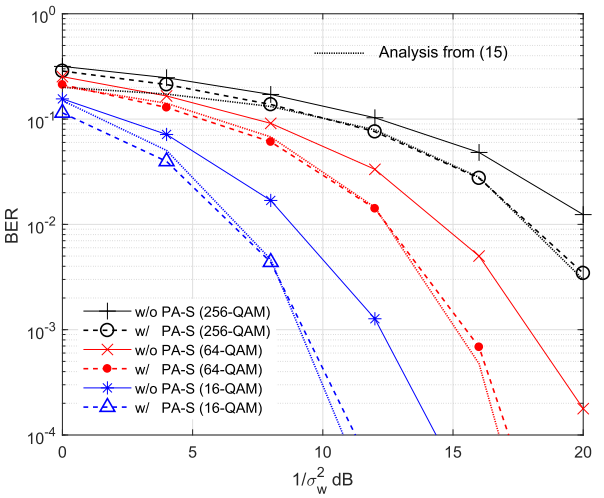

FIGURE 10. BER performance when $M = 20$, $\alpha = 1$, and $\delta = 1$ dB.

the fact that, as M increases, the BER of the PA-S-based STLC decreases faster than that of the conventional STLC without the PA-S. As presented in the figure, even with the additional switch insertion loss, the proposed PA-S can still provide significant performance gain, especially when M is large. However, when M is small, i.e., $M \leq 10$, the additional switch insertion loss hinders the PA-S from improving the BER performance. As M increases, the BER of the conventional STLC is saturated earlier than the PA-S-based STLC, because of the increment of the low gain PAs that rarely contribute to the decoding SNR without proper shuffling. On the other hand, as α increases from 0.5 in Fig. 8 to 1 in Fig. 9, the PA gains becomes more uneven, and thus the performance improvement by the PA-S is observed with the smaller number of PAs, i.e., the gain starts to appear when $M = 6$ and it increases as M increases.

In Fig. 10, the BER performance is evaluated for various σ_w^2's when $M = 20$, $\alpha = 1$, and $\delta = 1$ dB. As expected, even though the additional switch insertion loss exists, the substantial improvement of the BER performance is observed

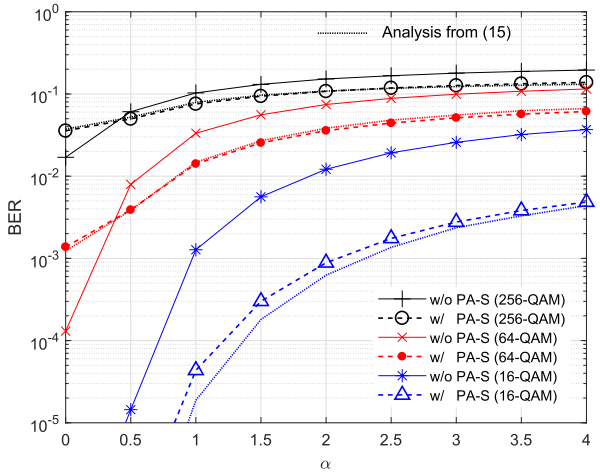

FIGURE 11. BER performance of a four transmit antenna system for various uneven factors α when $M = 20$, $1/\sigma_w^2 = 12$ dB, and $\delta = 1$ dB.

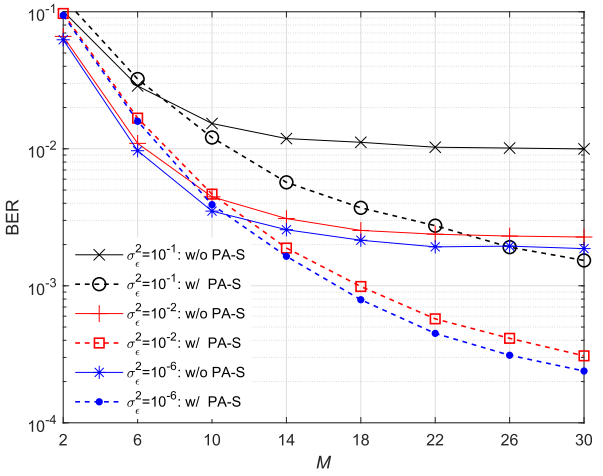

FIGURE 12. BER performance of STLC systems when $1/\sigma_w^2 = 8$ dB under CSI uncertainty. The exponential PA profile and 16-QAM are used, $\alpha = 0.5$, and $\delta = 1$ dB for PA-S.

by using the proposed PA-S regardless of σ_w^2. For example, to achieve 10^{-3} BER for 16-QAM transmission, the proposed method can achieve around 3 dB SNR gain. Here, the analysis in (15) is verified again.

In Fig. 11, BERs are evaluated for various values of α when $M = 20$, $1/\sigma_w^2 = 12$ dB, and $\delta = 1$ dB. When $\alpha = 0$, i.e., the PA gains are even, no performance improvement is obtained from the PA-S and the BER performance becomes rather worse due to the switch insertion loss. In general, as α increases, the performance of STLC schemes deteriorates because of the increment of small-gain PAs that degrade the effective channel gains at the receiver. However, the proposed PA-S method achieves almost constant performance gain regardless of α when $\alpha \geq 1$. Another interesting observation is that the higher gain is achieved from the proposed PA-S as the lower is the modulation size.

B. PA-S WITH CSI UNCERTAINTY IN TDD SYSTEMS

In the simulation of this subsection, uncertain CSI that is caused by the estimation at the transmitter in a TDD mode is assumed.

In Fig. 12, BER performance is shown when $1/\sigma_w^2 = 8$ dB under CSI uncertainty. Here, the exponential PA profile with $\alpha = 0.5$ is assumed and 16-QAM are used. Insertion loss $\delta = 1$ dB is considered for PA-S. From the results, it is observed that the STLC scheme is robust against the channel uncertainty, as reported in [12]. Furthermore, in the results, it is verified that the proposed PA-S STLC outperforms the conventional STLC without PA-S regardless of the channel uncertainty, especially, when the number of transmit antennas is sufficiently large, namely, $M > 10$ when $\sigma_\epsilon^2 \leq 10^{-2}$ and $M > 6$ when $\sigma_\epsilon^2 > 10^{-2}$.

In Fig. 13, all simulation parameters except the PA uneven parameter, i.e., more uneven PA gains with $\alpha = 1$ in this simulation, are the same as the parameters in Fig. 12. Indeed, the proposed PA-S STLC outperforms the conventional STLC without PA-S. Here, we further observe that the

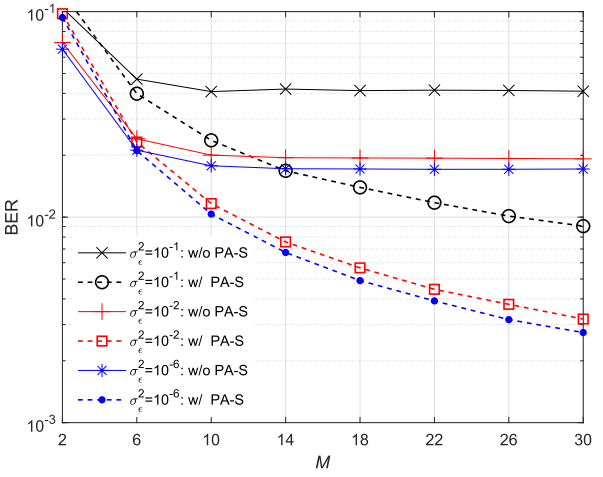

FIGURE 13. BER performance of STLC systems when $1/\sigma_w^2 = 8$ dB under CSI uncertainty. The exponential PA profile and 16-QAM are used, $\alpha = 1$, and $\delta = 1$ dB for PA-S.

minimum number of antennas such that the proposed PA-S STLC outperforms the conventional STLC is reduced. From this observation, we see that the PA-S is more effective (i.e., PA-S provides benefit even with small M) when the PA is more uneven. Moreover, it is observed that the BER of the conventional STLC is quickly saturated, while that of the proposed PA-S STLC is slowly saturated, as M increases.

In Fig. 14, BER performance is evaluated across CSI uncertainty, i.e., MSE σ_ϵ^2. In the results, again, it is verified that the STLC scheme is robust against channel uncertainty, and that the proposed PA-S STLC scheme outperforms the conventional STLC scheme without PA-S, regardless of the CSI uncertainty.

C. PA-S WITH CSI UNCERTAINTY IN FDD SYSTEMS

In this subsection, the limited feedback is considered for PA-S STLC system in an FDD mode. In the simulation, the codebook-based method is not used due to the design complexity in large-scale MIMO systems. Instead, a limited

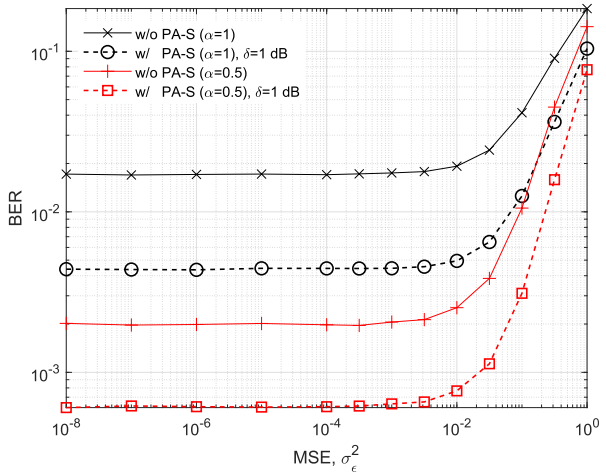

FIGURE 14. BER performance of STLC systems over MSE of channel estimation, i.e., σ_ϵ, when $M = 20$, $1/\sigma_w^2 = 8$ dB, and 16-QAM is used.

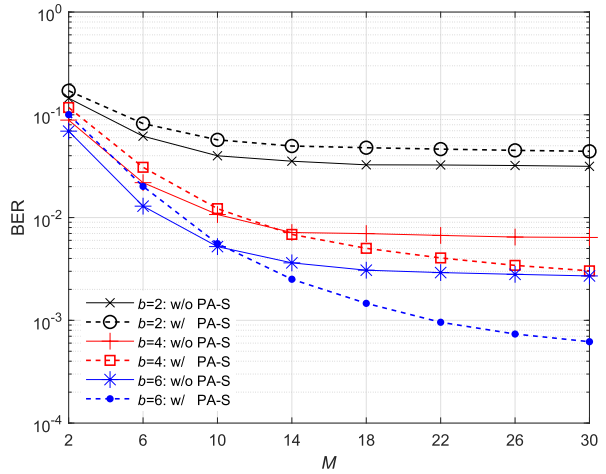

FIGURE 15. BER performance of STLC systems when $1/\sigma_w^2 = 8$ dB under CSI uncertainty. The exponential PA profile and 16-QAM are used, $\alpha = 0.5$, and $\delta = 1$ dB for PA-S.

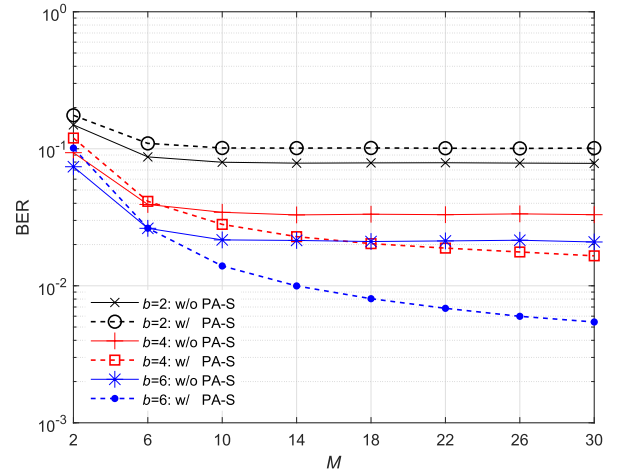

FIGURE 16. BER performance of STLC systems when $1/\sigma_w^2 = 8$ dB under CSI uncertainty. The exponential PA profile and 16-QAM are used, $\alpha = 1$, and $\delta = 1$ dB for PA-S.

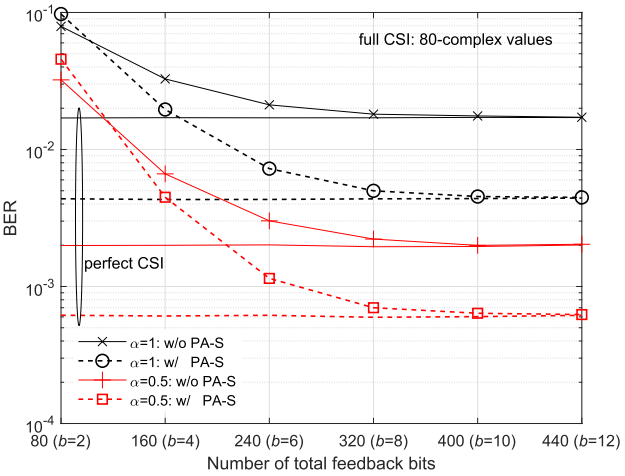

FIGURE 17. BER performance of STLC systems over MSE of channel estimation, i.e., σ_ϵ, when $M = 20$, $1/\sigma_w^2 = 8$ dB, $\delta = 1$ dB, and 16-QAM is used.

feedback scheme is employed, in which $b/2$ bits are used for representing the real and imaginary parts of each complex channel element, respectively, i.e. each complex channel is quantized with b bits. Thus, $2bM$-bit feedback information is used for the M-by-2 FDD STLC system. The Lloyd algorithm is used to optimally determine the quantization boundaries in terms of minimizing the mean square distortion [45].

In Fig. 15, the BER for 16-QAM symbol transmission is shown when $1/\sigma_w^2 = 8$ dB and $\alpha = 0.5$ under the CSI feedback scenario with various b. When the feedback information amount is insufficient, i.e., when $b = 2$, or when the number of transmit antennas is small, e.g., $M < 14$ for $b = 4$ and $M < 10$ for $b = 6$, the BER performance of the proposed STLC system with PA-S is worse than that of the conventional STLC system without PA-S. However, as M or b increases, the performance of the STLC with PA-S is gradually improved. Thus, the proposed method exhibits the better BER performance than the conventional STLC when $M > 14$ for $b = 4$ and $M > 10$ for $b = 6$, and the performance gain increases with the increment of M and b.

In Fig. 16, all simulation parameters except the PA uneven parameter are the same as the parameters in Fig. 15. We set $\alpha = 1$ for more uneven PA gains in this simulation. Similar results are observed to those in Fig. 15. Comparing to Figs. 15 and 16, we observe that the required minimum number of transmit antennas for achieving PA-S benefit is reduced from 14 to 6 for $b = 4$ and from 10 to 6 for $b = 6$. Thus, we can surmise even with the limited feedback that the PA-S works more effectively when the PA gains are more uneven.

To clarify the required feedback amount that provides the PA-S benefit, the BER performances are compared for varying number of total feedback bits, i.e., $2Mb$, in Fig. 17. Here, we set $M = 20$ and $1/\sigma_w^2 = 8$ dBm. From the numerical results, we observe that the proposed PA-S STLC has the lower BER performance than the conventional STLC without PA-S, if $b \geq 4$. In other words, in order to achieve BER

performance gain through the proposed PA-S, at least two-bit quantization is required to represent the real or imaginary part of one complex channel element.

V. CONCLUSION

In this paper, a novel PA-S method was proposed for an STLC system with uneven PA gains. The optimal PA-S scheme was designed to maximize the decoding SNR of STLC symbols. Therefore, the proposed PA-S method can improve the performance of STLC systems in the presence of the intentional or unintentional variation of PA gains. The performance improvement by the proposed PA-S was verified by numerical simulations. From the numerical results, it was shown that the proposed PA-S can provide benefit regardless of channel state information uncertainty, especially with a large number of transmit antennas.

APPENDIX
OPTIMAL PA-S MAXIMIZING THE EFFECTIVE CHANNEL GAIN OF STLC

This section shows that $\lambda(i_m)$ in (10a) is maximized when g_m is mapped to the transmit antenna with the mth largest channel gain. Note that the PA gains are sorted in descending order, i.e. $g_1 \geq g_2 \geq \cdots \geq g_M$. When $M = 2$, we can compute the difference of $\lambda(\{1, 2\})$ and $\lambda(\{2, 1\})$ from (9) as follows:

$$\begin{aligned}&\lambda(\{1,2\}) - \lambda(\{2,1\}) \\ &\quad = (g_1\|\boldsymbol{h}_1\| + g_2\|\boldsymbol{h}_2\|) - (g_1\|\boldsymbol{h}_2\| + g_2\|\boldsymbol{h}_1\|) \\ &\quad = (g_1 - g_2)(\|\boldsymbol{h}_1\| - \|\boldsymbol{h}_2\|). \end{aligned} \tag{A.1}$$

From (A.1), $\lambda(i_m)$ is maximized if g_1 is mapped to $\max(\|\boldsymbol{h}_1\|, \|\boldsymbol{h}_2\|)$ and g_2 is mapped to $\min(\|\boldsymbol{h}_1\|, \|\boldsymbol{h}_2\|)$. When M transmit antennas are used, suppose that $\|\boldsymbol{h}_k\| > \|\boldsymbol{h}_l\|$ for $k > l$. Then, from (A.1), we may write

$$\begin{aligned}&\lambda(\{i_1, \cdots, i_{m_1}, k, \cdots, i_{m_2}, l, \cdots, i_M\}) \\ &\qquad > \lambda(\{i_1, \cdots, i_{m_1}, l, \cdots, i_{m_2}, k, \cdots, i_M\}). \end{aligned} \tag{A.2}$$

From (A.2), if there exist any indices l and k satisfying $\|\boldsymbol{h}_k\| > \|\boldsymbol{h}_l\|$ for $k > l$, the effective channel gain $\lambda(i_m)$ is increased by switching l and k, i.e. switching $\|\boldsymbol{h}_l\|$ and $\|\boldsymbol{h}_k\|$. By repeating this procedure, the effective channel gain $\lambda(i_m)$ is maximized when the channel gains $\|\boldsymbol{h}_1\|, \|\boldsymbol{h}_2\|, \cdots, \|\boldsymbol{h}_M\|$ are sorted in descending order, i.e. $\|\boldsymbol{h}_{s,1}\| \geq \|\boldsymbol{h}_{s,2}\| \geq \cdots \geq \|\boldsymbol{h}_{s,M}\|$, where $\|\boldsymbol{h}_{s,m}\|$ is the mth largest channel gain. This concludes that $\lambda(i_m)$ is maximized when g_m is mapped to $\|\boldsymbol{h}_{s,m}\|$ denoting the transmit antenna with the mth largest channel gain.

REFERENCES

[1] S. Shim, K. Kim, and C. Lee, "An efficient antenna shuffling scheme for a DSTTD system," *IEEE Commun. Lett.*, vol. 9, no. 2, pp. 124–126, Feb. 2005.

[2] J. Joung, E. R. Jeong, and Y. H. Lee, "A computationally efficient criterion for antenna shuffling in DSTTD systems," *IEEE Commun. Lett.*, vol. 11, no. 9, pp. 732–734, Sep. 2007.

[3] Y. Yu, S. Kerouedan, and J. Yuan, "Transmit antenna shuffling for quasi-orthogonal space-time block codes with linear receivers," *IEEE Commun. Lett.*, vol. 10, no. 8, pp. 596–598, Aug. 2006.

[4] V. Sharma and S. Sharma, "Novel linear decodable QO-STBC for four transmit antennas with transmit antenna shuffling," *Wireless Pers. Commun.*, vol. 82, no. 1, pp. 47–59, May 2015.

[5] J. Joung, C. K. Ho, and S. Sun, "Power amplifier switching (PAS) for energy efficient systems," *IEEE Wireless Commun. Lett.*, vol. 2, no. 1, pp. 14–17, Feb. 2013.

[6] J. Joung, C. K. Ho, and S. Sun, "Power amplifier switching/selection (PAS) for energy efficient MIMO systems," in *Proc. IEEE Global Commun. Conf. (GLOBECOM)*, Austin, TX, USA, Dec. 2014, pp. 1272–1277.

[7] O. Apilo, M. Lasanen, and A. Mämmelä, "Unequal power amplifier dimensioning for adaptive massive MIMO base stations," in *Proc. IEEE Veh. Technol. Conf. (VTC)*, Glasgow, Scotland, May 2016, pp. 1–6.

[8] H. Liu *et al.*, "A wideband analog-controlled variable-gain amplifier with dB-linear characteristic for high-frequency applications," *IEEE Trans. Microw. Theory Techn.*, vol. 64, no. 2, pp. 533–540, Feb. 2016.

[9] J. Joung, "Power efficient 2×1 space–time block code system with antenna shuffling," *IET Electron. Lett.*, vol. 54, no. 7, pp. 458–460, Feb. 2018.

[10] J. Joung and J. Choi, "Transmit antenna shuffling for orthogonal STBC systems with uneven transmit antenna gains," *IEEE Trans. Veh. Technol.*, vol. 67, no. 7, pp. 6673–6678, Jul. 2018.

[11] J. Joung, "Space–time line code," *IEEE Access*, vol. 6, pp. 1023–1041, Feb. 2018.

[12] J. Joung, "Space–time line code for massive MIMO and multiuser systems with antenna allocation," *IEEE Access*, vol. 6, pp. 962–979, Feb. 2018.

[13] J. Joung, "Energy efficient space-time line coded regenerative two-way relay under per-antenna power constraints," *IEEE Access*, vol. 6, pp. 47026–47035, Sep. 2018.

[14] J. Joung and E.-R. Jeong, "Multiuser space-time line code with optimal and suboptimal power allocation methods," *IEEE Access*, vol. 6, pp. 51766–51775, Oct. 2018.

[15] W. C. Jakes, *Microwave Mobile Communications*. New York, NY, USA: Wiley, 1994.

[16] C. Chayawan and V. A. Aalo, "Average error probability of digital cellular radio systems using MRC diversity in the presence of multiple interferers," *IEEE Trans. Wireless Commun.*, vol. 2, no. 5, pp. 860–864, Sep. 2003.

[17] S. Roy and P. Fortier, "Maximal-ratio combining architectures and performance with channel estimation based on a training sequence," *IEEE Trans. Wireless Commun.*, vol. 3, no. 4, pp. 1154–1164, Jul. 2004.

[18] W. M. Gifford, M. Z. Win, and M. Chiani, "Diversity with practical channel estimation," *IEEE Trans. Wireless Commun.*, vol. 4, no. 4, pp. 1935–1947, Jul. 2005.

[19] K. S. Ahn and R. W. Heath, Jr., "Performance analysis of maximum ratio combining with imperfect channel estimation in the presence of cochannel interferences," *IEEE Trans. Wireless Commun.*, vol. 8, no. 3, pp. 1080–1085, Mar. 2009.

[20] T. K. Y. Lo, "Maximum ratio transmission," in *Proc. IEEE Int. Conf. Commun. (ICC)*, Vancouver, BC, Canada, Jun. 1999, pp. 1210–1314.

[21] J. K. Cavers, "Single-user and multiuser adaptive maximal ratio transmission for Rayleigh channels," *IEEE Trans. Veh. Technol.*, vol. 49, no. 6, pp. 2043–2050, Nov. 2000.

[22] Y. Chen and C. Tellambura, "Performance analysis of maximum ratio transmission with imperfect channel estimation," *IEEE Commun. Lett.*, vol. 9, no. 4, pp. 322–324, Apr. 2005.

[23] V. Tarokh, N. Seshadri, and A. R. Calderbank, "Space–time codes for high data rate wireless communication: Performance criterion and code construction," *IEEE Trans. Inf. Theory*, vol. 44, no. 2, pp. 744–764, Mar. 1998.

[24] S. M. Alamouti, "A simple transmit diversity technique for wireless communications," *IEEE J. Sel. Areas Commun.*, vol. 16, no. 8, pp. 1451–1458, Oct. 1998.

[25] V. Tarokh, H. Jafarkhani, and A. R. Calderbank, "Space–time block codes from orthogonal designs," *IEEE Trans. Inf. Theory*, vol. 45, no. 5, pp. 1459–1467, Jul. 1999.

[26] V. Tarokh, H. Jafarkhani, and A. R. Calderbank, "Space-time block coding for wireless communications: Performance results," *IEEE J. Sel. Areas Commun.*, vol. 17, no. 3, pp. 451–460, Mar. 1999.

[27] C. Chang and P. Chang, "Innovative micromachined microwave switch with very low insertion loss," *Sens. Actuators A, Phys.*, vol. 79, no. 1, pp. 71–75, Jan. 2000.

[28] K. Yamamoto *et al.*, "A 2.4-GHz-band 1.8-V operation single-chip Si-CMOS T/R-MMIC front-end with a low insertion loss switch," *IEEE J. Solid-State Circuits*, vol. 36, no. 8, pp. 1186–1197, Aug. 2001.

[29] C. Tinella, J. M. Fournier, D. Belot, and V. Knopik, "A 0.7 dB insertion loss CMOS-SOI antenna switch with more than 50 dB isolation over the 2.5 to 5 GHz band," in *Proc. 28th Eur. Solid-State Circuits Conf.*, Florence, Italy, 2002, pp. 483–486.
[30] W. Cai, C. Li, and S. Luan. (Jan. 2017). "SOI RF switch for wireless sensor network." [Online]. Available: https://arxiv.org/abs/1701.01763
[31] P. Gao and C. Tepedelenlioglu, "SNR estimation for nonconstant modulus constellations," *IEEE Trans. Signal Process.*, vol. 53, no. 3, pp. 865–870, Mar. 2005.
[32] J. Shi, Q. Luo, and M. You, "An efficient method for enhancing TDD over the air reciprocity calibration," in *Proc. IEEE Wireless Commun. Netw. Conf. (WCNC)*, Quintana Roo, Mexico, Mar. 2011, pp. 339–344.
[33] J. Vieira, F. Rusek, and F. Tufvesson, "Reciprocity calibration methods for massive MIMO based on antenna coupling," in *Proc. IEEE Global Commun. Conf. (GLOBECOM)*, Austin, TX, USA, Dec. 2014, pp. 3708–3712.
[34] A. F. Naguib, V. Tarokh, N. Seshadri, and A. R. Calderbank, "A space-time coding modem for high-data-rate wireless communications," *IEEE J. Sel. Areas Commun.*, vol. 16, no. 8, pp. 1459–1478, Oct. 1998.
[35] D. J. Love, R. W. Heath, Jr., W. Santipach, and M. L. Honig, "What is the value of limited feedback for MIMO channels?" *IEEE Commun. Mag.*, vol. 42, no. 10, pp. 54–59, Oct. 2004.
[36] J. Mo and R. W. Heath, Jr., "Limited feedback in single and multi-user MIMO systems with finite-bit ADCs," *IEEE Trans. Wireless Commun.*, vol. 17, no. 5, pp. 3284–3297, May 2018.
[37] D. J. Love, R. W. Heath, Jr., and T. Strohmer, "Grassmannian beamforming for multiple-input multiple-output wireless systems," in *Proc. IEEE Int. Conf. Commun. (ICC)*, Anchorage, AK, USA, Jun. 2003, pp. 2618–2622.
[38] D. J. Love and R. W. Heath, Jr., "Limited feedback unitary precoding for spatial multiplexing systems," *IEEE Trans. Inf. Theory*, vol. 51, no. 8, pp. 2967–2976, Aug. 2005.
[39] H. Seleem, A. I. Sulyman, and A. Alsanie, "Hybrid precoding-beamforming design with Hadamard RF codebook for mmWave large-scale MIMO systems," *IEEE Access*, vol. 5, pp. 6813–6823, Mar. 2017.
[40] T. Jiang, M. Song, X. Zhao, and X. Liu, "A codebook-adaptive feedback algorithm for cellular-based positioning," *IEEE Access*, vol. 6, pp. 32109–32116, Jun. 2018.
[41] Y. Ren, Y. Wang, C. Qi, and Y. Liu, "Multiple-beam selection with limited feedback for hybrid beamforming in massive MIMO systems," *IEEE Access*, vol. 5, pp. 13327–13335, Feb. 2017.
[42] W. Huang, Y. Huang, W. Xu, and L. Yang, "Beam-blocked channel estimation for FDD massive MIMO with compressed feedback," *IEEE Access*, vol. 5, pp. 11791–11804, 2017.
[43] F. Zheng *et al.*, "An efficient CSI feedback scheme for dual-polarized massive MIMO," *IEEE Access*, vol. 6, pp. 23420–23430, Mar. 2018.
[44] C. Xu, R. Ye, Y. Huang, S. He, and C. Zhang, "Hybrid precoding for broadband millimeter-wave communication systems with partial CSI," *IEEE Access*, vol. 5, pp. 15142–15151, Aug. 2018.
[45] Y. Linde, A. Buzo, and R. M. Gray, "An algorithm for vector quantizer design," *IEEE Trans. Commun.*, vol. 28, no. 1, pp. 84–95, Jan. 1980.

JINGON JOUNG (S'03–M'07–SM'15) received the B.S. degree in radio communication engineering from Yonsei University, Seoul, South Korea, in 2001, and the M.S. and Ph.D. degrees in electrical engineering and computer science from the Korea Advanced Institute of Science and Technology (KAIST), Daejeon, South Korea, in 2003 and 2007, respectively.

He was a Post-Doctoral Research Scientist with KAIST in 2017. He is currently an Assistant Professor with the School of Electrical and Electronics Engineering, Chung-Ang University (CAU), Seoul, where he is also the Principal Investigator of the Wireless Systems Laboratory. Before joining CAU in 2016, he was a Scientist with the Institute for Infocomm Research, Agency for Science, Technology and Research, Singapore. He is also a Post-Doctoral Fellow with UCLA, CA, USA. His research activities are in the areas of multiuser systems, multiple-input multiple-output communications, and cooperative systems. His current research areas/interests include STLC, V2X, UAV communications, and machine learning algorithms.

Dr. Joung was a recipient of the First Prize of the Intel-ITRC Student Paper Contest in 2006 and the Best Paper Award from the Korean Institute of Communications and Information Sciences Conference in 2018 (Winter and Summer). He is recognized as the Exemplary Reviewers of the IEEE COMMUNICATIONS LETTERS in 2012 and the IEEE WIRELESS COMMUNICATIONS LETTERS in 2012 and 2013. He served as the Guest Editor for the IEEE ACCESS for the special section Recent Advanced in Full-Duplex Radios and Networks in 2016. He has been serving on the Editorial Board of the *APSIPA Transactions on Signal and Information Processing* since 2014. He is currently serving as an Associate Editor for the IEEE TRANSACTIONS ON VEHICULAR TECHNOLOGY, and as a Guest Editor for the *MDPI Electronics* for the special issue IoT in 5G.

JIHOON CHOI (S'99–M'04–SM'18) received the B.S., M.S., and Ph.D. degrees from the Korea Advanced Institute of Science and Technology (KAIST), Daejeon, South Korea, in 1997, 1999, and 2003, respectively. From 2003 to 2004, he was with the Department of Electrical and Computer Engineering, The University of Texas at Austin, where he performed research on MIMO-OFDM systems. From 2004 to 2008, he was with Samsung Electronics, South Korea, where he was involved in the developments of radio access stations for M-WiMAX and base stations for CDMA 1xEV-DO Rev.A/B. Since 2008, he has been with the School of Electronics, Telecommunication, and Computer Engineering, Korea Aerospace University, where he is currently a Professor. His research interests include MIMO communications, wireless information and power transfer, wireless secure communications, UAV-assisted wireless network design, signal processing algorithms, modem design for future cellular networks, wireless LANs, sensor networks, IoT, relays, and digital broadcasting systems.